Acta Materialia 103 (2016) 211–216

Contents lists available at ScienceDirect

Acta Materialia

journal homepage: www.elsevier.com/locate/actamat

Magnetic properties of bulk, and rapidly solidified nanostructured $(Nd_{1-x}Ce_x)_2Fe_{14-y}Co_yB$ ribbons

Arjun K. Pathak [a,*], M. Khan [a,1], K.A. Gschneidner Jr. [a,b], R.W. McCallum [a], L. Zhou [a], K. Sun [a], M.J. Kramer [a,b], V.K. Pecharsky [a,b]

[a] The Ames Laboratory, U.S. Department of Energy, Iowa State University, Ames, IA 50011-3020, USA
[b] Department of Materials Science and Engineering, Iowa State University, Ames, IA 50011-2300, USA

ARTICLE INFO

Article history:
Received 17 July 2015
Received in revised form 23 September 2015
Accepted 25 September 2015
Available online 6 November 2015

Keywords:
Permanent magnet
Melt spun ribbons
Maximum energy product

ABSTRACT

Magnetic properties of Ce and Co co-doped $(Nd_{1-x}Ce_x)_2Fe_{14-y}Co_yB$ compounds have been investigated both in bulk polycrystalline and rapidly solidified nanostructured ribbon forms. For certain Ce concentrations the materials exhibit spin re-orientation transitions below 140 K. The Curie temperatures, saturation magnetizations, and other magnetic properties relevant for applications as permanent magnets are controlled by Ce and Co substitutions for Nd and Fe, respectively. Most importantly, the results show that Ce, Co co-doped compounds are excellent replacements for several Dy-based high performance permanent magnets (dysprosium is one of the critical elements and is, therefore, in short supply). The high temperature (>375 K) magnetic properties for Nd–Ce–Fe–Co–B based alloys show promise not only as a replacement for Dy-doped $Nd_2Fe_{14}B$ permanent magnets, but the new alloys also require significantly lower amounts of Nd, which too is the critical element that can be replaced by a more abundant Ce.

© 2015 Acta Materialia Inc. Published by Elsevier Ltd. All rights reserved.

1. Introduction

The discovery of $Nd_2Fe_{14}B$ based permanent magnets (PMs) in the 1980's [1] revolutionized the permanent magnet industry, and made it possible for crucial energy efficient technologies like wind turbines, hybrid-vehicle-motors, and other come into existence. It is well-known that Nd–Fe–B based PMs have excellent magnetic properties at room temperature but exhibit poor high temperature (T > 400 K) performance. For efficient applications in technologies like electric drive motors, and wind turbines, the magnetic properties must be retained at T > 400 K, and hence the addition of significant amounts of Dy is required. Unfortunately, both Dy and Nd are critical elements based on supply risk versus significance to clean energy. Keeping this in mind, it is extremely important to develop PMs that are rare earth (RE) free, or at least have reduced amounts of the critical REs Dy and Nd, and hence there has been an intense worldwide research effort to develop RE free (or reduced RE) based PMs.

It is well know that the magnetic properties of RE-Fe-B based permanent magnets are strongly dependent on materials processing, grain size distribution, and thereby their microstructure. Among them controlling microstructure by varying the wheel speed, quenching rate in melt spun ribbons [2], and grain boundary diffusion process in sintered magnets [3] are common practices. It was found that addition of Ti or TiC enhances glass-forming ability [4], reduces grain size, and produces a uniform microstructure [5]. Similarly, it was reported that substitution of Nb for Fe increases thermal stability of melt-spun ribbons and thereby increases the coercivity [6]. In addition, several rare earth metals, including, La, Ce, Pr, Eu and Dy, have been substituted for Nd, and their hard magnetic properties have been studied [7–10]. Among the lanthanides, Ce is the most abundant RE metal and often exhibits a mixed valency when alloyed with other elements. Recently, various attempts have been made to prepare Ce doped $RE_2Fe_{14}B$ based alloys [11–15]. Li et al. [16] reported that the substitution of Ce for Nd in $(Nd_{12x}Ce_x)Fe_{82}B_6$ ribbons decreases both intrinsic coercivity, Hci, and maximum energy product, (BH)max. The ribbons exhibit a poor demagnetization curve in the second quadrant for Ce concentrations in excess of 10 at.%, i.e. when x exceeds 1.2. Another study of Ce substitution for didymium (Di, which is a mixture of Pr and Nd at natural abundance) in Di-Fe-B shows that the remanent magnetization Br, (BH)max,

* Corresponding author.
E-mail address: pathak138@ameslab.gov (A.K. Pathak).
[1] Current address: Department of Physics, Miami University, Oxford, OH-45056, USA.

http://dx.doi.org/10.1016/j.actamat.2015.09.049
1359-6454/© 2015 Acta Materialia Inc. Published by Elsevier Ltd. All rights reserved.

and Hci decrease linearly, except for a minor anomaly in Hci observed at x_{Ce} = 0.24 in $(Di_{1x}Ce_x)_{27.5}Dy_3Al_{0.1}Cu_{0.1}Fe_{13.8}B$, where $CeFe_2$ phase forms for x ≥ 0.24 [17]. Moreover, it was reported that substitution of Co for Fe in $Nd_2Fe_{14}B$ increases T_C [18]. Even though the Co moment (1.6 μ_B) is lower than that of Fe atom (2.2 μ_B), the saturation magnetization is enhanced for Co additions up to 30%, and then decreased for higher Co concentrations in $Nd_2Fe_{14-x}Co_xB$ [18].

Recently, we showed that by simultaneous partial replacements of Nd by Ce and Fe by Co in $(Nd_{1-x}Ce_x)_2Fe_{14-y}Co_yB$ it is possible to develop high performance PMs [19]. The Hci values of melt spun ribbons, hot pressed, and die upset magnets of $(Nd_{0.8}Ce_{0.2})_{2.4}Fe_{12}Co_2B$ are respectively, 17.7, 13.7, and 9.4 kOe, and the corresponding (BH)max values are 12.6, 12.8 and 31 MGOe. Although permanent magnetic properties of some of Ce-doped $Nd_2Fe_{14}B$ alloys had been reported in Refs. [11–15,19], high temperature magnetic properties of $(Nd_{1-x}Ce)_2Fe_{14}B$ including those with a high concentration of Ce and low amounts of Co doped $Nd_2Fe_{14}B$ are yet to be examined.

From both scientific and application points of view it is important to understand how the magnetic properties of $(Nd_{1-x}Ce_x)_2Fe_{14-y}Co_yB$ change from bulk to nanostructured compounds. In this letter, we report on an experimental study on the magnetic properties of selected bulk polycrystalline, and rapidly solidified nanostructured $(Nd_{1-x}Ce_x)_2Fe_{14-y}Co_yB$ compounds at temperatures up to 500 K. We show that by substituting up to 50% Ce for Nd can result in enhanced PM properties at high temperatures. The values of Hci, (BH)max at 300 K, and T_C for $(Nd_{0.8}Ce_{0.2})_2Fe_{12}Co_2B$ and $(Nd_{0.5}Ce_{0.5})_2Fe_{13}CoB$ alloys were found to be 7.7 kOe, 16 MGOe, 695 K, and 8 kOe, 14.6 MGOe, 590 K, respectively. More interesting, the substitution of both Ce for Nd, and Co for Fe results in the synergistic effect between Co and $Ce^{3.44+}$ in the rapidly solidified ribbons that leads to better Hci and (BH)max values than those of commercial Dy containing Nd–Fe–B ribbons at T ≥ 450 K.

2. Experimental methods

Alloys (approximately 15 g each) were prepared by arc melting followed by drop cast using through a ~9.6 mm diameter orifice at the following stoichiometries $(Nd_{1-x}Ce_x)_2Fe_{14}B$, $(Nd_{0.8}Ce_{0.2})_2Fe_{14-y}Co_yB$, $(Nd_{0.8}Ce_{0.2})_2Fe_{14-y}Co_yB$ + 2.5% ZrC, $(Nd_{0.5}Ce_{0.5})_2Fe_{14-y}Co_yB$ using high purity (99.9 + wt.%) Nd and Ce obtained from the Materials Preparation Center at the Ames Laboratory. In case of the ZrC containing alloys, Zr and C at a concentration equivalent to 2.5 wt% ZrC were added during the melting. The drop cast alloys were annealed at 1000 °C for 3 days, and found to be ~98% $Nd_2Fe_{14}B$ phase with minor α-Fe phase. The melt-spun ribbons were prepared by induction melting ingots in a quartz crucible in 1/3 atm of high purity He gas and then ejected at 125 torr overpressure onto a copper chill wheel rotating at a tangential speed of ~25 m/s. The as-spun ribbons were annealed in helium atmosphere at different temperatures, and times. The optimum temperature and time were found to be 600 °C, and 20 min, respectively. The magnetization measurements were performed in a Physical Property Measurement System (PPMS) made by Quantum Design Inc in magnetic field up to 50 kOe and temperatures up to 1000 K. Transmission electron microscopy (TEM) samples were prepared by mechanical polishing followed by low voltage short-time Ar ion milling with liquid nitrogen cooling. An FEI Tecnai F20 (200 kV, FEG) TEM was used for microstructural characterization.

3. Results and discussion

The magnetization, M, of drop cast $(Nd_{1-x}Ce_x)_2Fe_{14}B$ alloys measured as a function of temperature in a 1 kOe magnetic field is shown in Fig. 1a. Most of the compounds undergo two transitions: a high temperature ferromagnetic (FM) to paramagnetic (PM) one that occurs at Curie temperatures, T_C, exceeding 420 K (Fig. 1a), and a low temperature spin re-orientation transition at T_{SR} ≤ 135 K (Fig. 1b, and inset in Fig. 1b). An additional anomaly at T ≅ 315 K is observed for 0.2 ≤ x ≤ 0.3. The T_C decreases with increasing Ce concentration, and it varies from 580 K for x = 0 to 546 K for x = 0.2 to 420 K for x = 1 (inset, Fig. 1a). The T_{SR} also decreases with Ce concentration, and it disappears at x = 1 (Fig. 1b). The decrease in T_C with increasing Ce concentration can be attributed to the decreasing magnetic exchange interaction with Ce substitution. An earlier report based on a scanning electron microscopy study suggests that the anomaly in M(T) for 0.2 ≤ x ≤ 0.3 at T < T_C is associated with phase segregation i.e. with the presence of two phases both having the 2:14:1 type structure with slightly different Ce concentrations [20], where a small anomaly in room temperature *c* lattice parameter of the tetragonal phase is also observed. The T_C also deviates from the nearly linear dependence on x near this concentration (inset, Fig. 1a). The magnetization shown for selected drop cast $(Nd_{1-x}Ce_x)_2Fe_{14}B$ alloys as a function of magnetic field in Fig. 1c represents typical soft magnetic behavior with negligible coercivity, compared to hard magnetism of melt spun ribbons prepared from the same alloys [19]. The saturation magnetization of the drop cast alloys is close to that of the melt spun ribbons, and it decreases with increasing Ce concentration (Fig. 1c, inset).

The room temperature magnetic hysteresis loops for melt-spun ribbons of $Nd_2Fe_{14}B$ and $(Nd_{0.8}Ce_{0.2})_2Fe_{14}B$ are shown in Fig. 2a, where the intrinsic coercivity Hci increases from 8.3 for x = 0 to 10 kOe for x = 0.2. However, the maximum energy product (BH)max decreases from 13.8 to 11 MGOe for the respective melt spun ribbons at room temperature, which is due to poor demagnetization curve in the second quadrant (Fig. 2a). One of the possible reasons of the poor demagnetization curve may be due to the non-uniform magnetization reversal in the grains of melt spun ribbons which results from increase of soft phase with Ce substitution as suggested in Ref. [21]. The magnetization as a function of magnetic field was measured for both $Nd_2Fe_{14}B$, and $(Nd_{0.8}Ce_{0.2})_2Fe_{14}B$ up to 500 K. The obtained values of Hci, (BH)max and Br from M(H) measurement are plotted in Fig. 2b–d, respectively. The Hci of 20% Ce substitution in $Nd_2Fe_{14}B$ has a higher Hci from 300 to 500 K, but both (BH)max, and Br are smaller at all temperatures.

Typical transmission electron microscopy images of $(Nd_{1-x}Ce_x)_2Fe_{14}B$ are shown in Fig. 3. The grain size (~20 nm on average) remains unchanged from wheel side to free side for $Nd_2Fe_{14}B$ (Fig. 3a–b), but there is a significant difference in the grain size for Ce doped samples (Fig. 3c–d). The grain size near the free side is on the order of hundreds of nanometers; but the grains near the wheel side are only about 20–50 nm for $(Nd_{0.8}Ce_{0.2})_2Fe_{14}B$ (not shown in Fig. 3). The grain size near the wheel side for $(Nd_{0.75}Ce_{0.25})_2Fe_{14}B$ is about 50–100 nm (Fig. 3c). However, at the free side (Fig. 3d), there is a significant increase in the grain size. Fig. 3e–g show microprobe WDS (wavelength dispersion spectroscopy) analysis for $(Nd_{0.75}Ce_{0.25})_2Fe_{14}B$ melt spun ribbons from wheel sides (left) to free side (right). The microprobe WDS results shows nearly constant concentrations of Nd, Ce and Fe throughout the cross-section of ribbons, and the composition is very close to 2:14:1, where the ratios of Fe/RE and Nd/Ce are about 7, and 3, respectively, for $(Nd_{0.75}Ce_{0.25})_2Fe_{14}B$ (Fig. 3g).

High Curie temperature is one of the desired properties for permanent magnet applications. Considering previous studies reporting increased T_C by substituting Co for Fe in $Nd_2Fe_{14}B$ [18,22], Co was substituted for Fe in $(Nd_{1-x}Ce_x)_2Fe_{14-y}Co_yB$ compounds for x = 0.2, 0.25, 0.3, and 0.5. Here we show the data for $(Nd_{1-x}Ce_x)_2Fe_{14-y}Co_yB$ with x = 0.2, and 0.5, and y = 0 to 4. The magnetization as a function of temperature for $(Nd_{0.8}Ce_{0.2})_2Fe_{14-y}Co_yB$ measured in 1 kOe

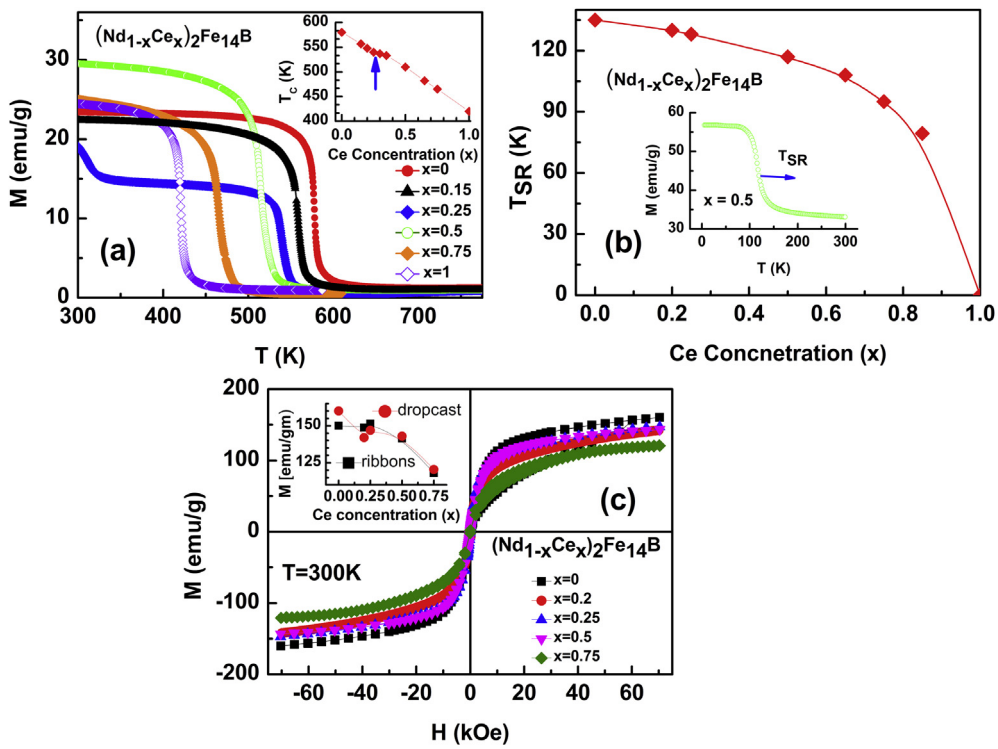

Fig. 1. (a) Magnetization of drop cast $(Nd_{1-x}Ce_x)_2Fe_{14}B$ alloys measured as a function of temperature in 1 kOe magnetic field. (b) Variation of spin reorientation transition temperature, T_{SR}, as a function of Ce concentration in $(Nd_{1-x}Ce_x)_2Fe_{14}B$. (c) Magnetization as a function of magnetic field for $(Nd_{1-x}Ce_x)_2Fe_{14}B$ drop cast alloys at 300 K. The insets in (a), (b) and (c) show, respectively, the Curie temperature as a function of Ce concentration; low temperature magnetization of drop cast $(Nd_{0.5}Ce_{0.5})_2Fe_{14}B$ measured in 1 kOe magnetic field; and saturation magnetization for both ribbons and drop cast alloys as a function of Ce concentration.

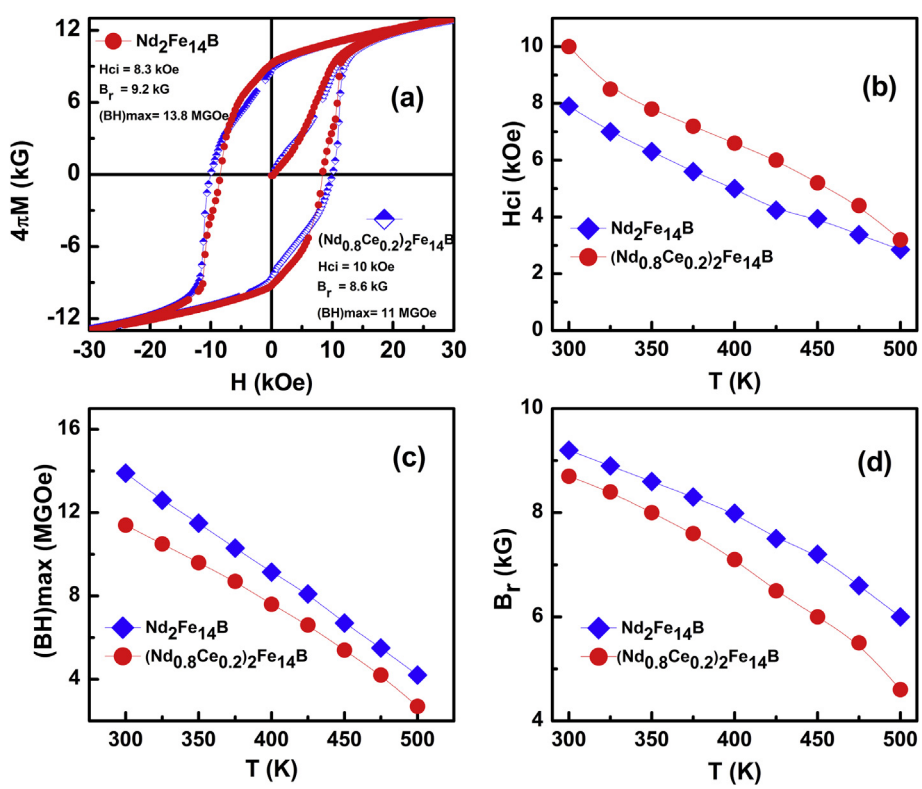

Fig. 2. (a) Magnetization of melt spun ribbons of $(Nd_{1-x}Ce_x)_2Fe_{14}B$ with x = 0, and 0.2 measured at 300 K as a function of magnetic field; (b) Intrinsic coercivity Hci; (c) maximum energy product (BH)max; and (d) remanence magnetization Br as functions of temperature for melt spun ribbons of $(Nd_{1-x}Ce_x)_2Fe_{14}B$ with x = 0, and 0.2.

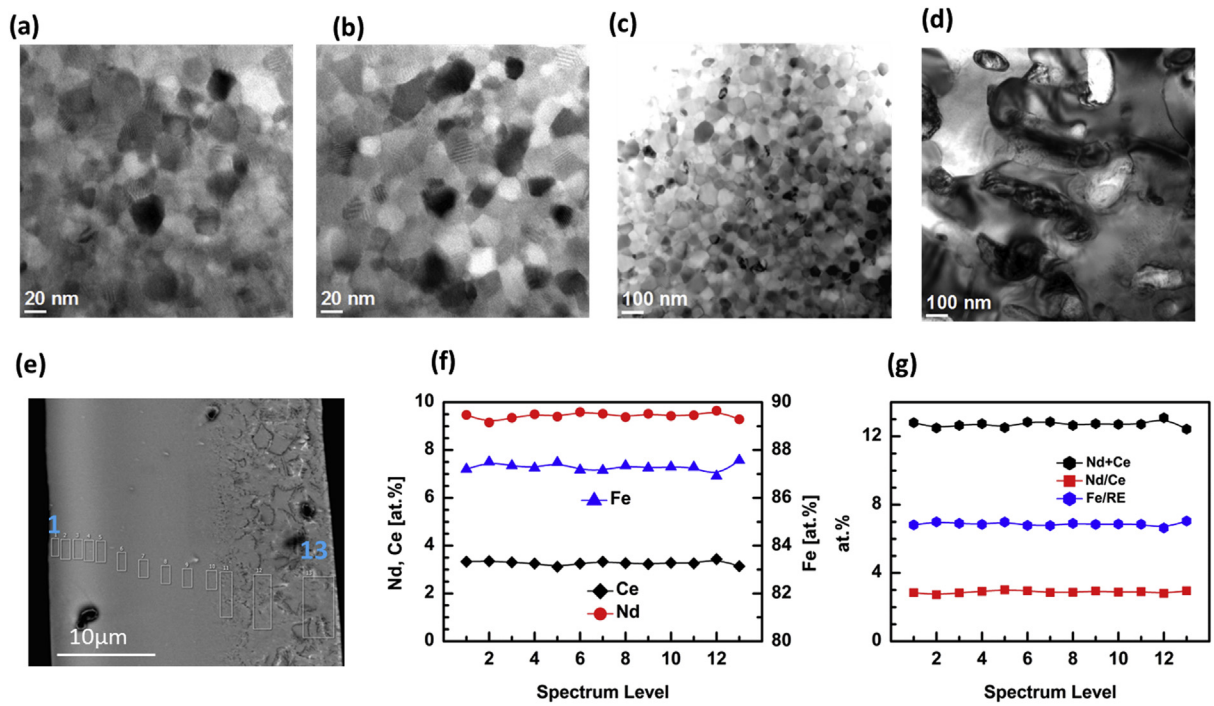

Fig. 3. Transmission electron microscopy (TEM) micrographs of the wheel side (a), the free side (b) of $Nd_2Fe_{14}B$ and wheel side (c), free side (d) of $(Nd_{0.75}Ce_{0.25})_2Fe_{14}B$ melt spun ribbons. (e) Cross-section area of ribbon from wheel side (left end) (1) to free side right end (13). The spectrum level numbers 1 to 13 are the equidistant points across the ribbons from point 1 to point 13. (f, g) Microprobe WDS (wavelength dispersion spectroscopy) analysis from the wheel side (1) to free side (13) for $(Nd_{0.75}Ce_{0.25})_2Fe_{14}B$ melt spun ribbon shown in Fig. 3(e).

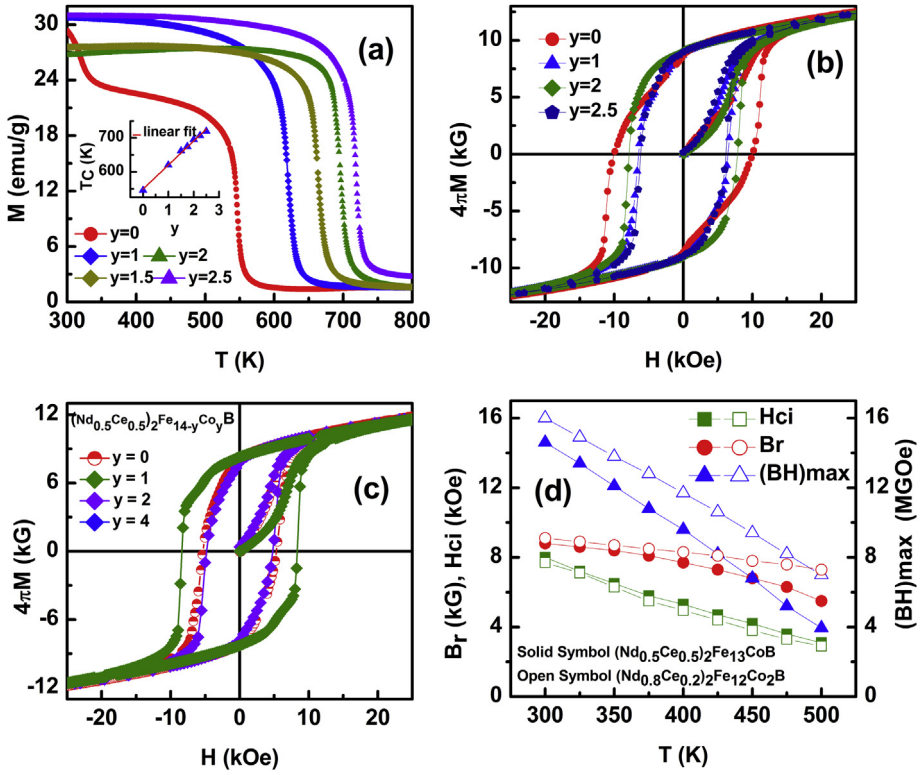

Fig. 4. (a) Magnetization as a function of temperature for melt spun $(Nd_{0.8}Ce_{0.2})_2Fe_{14-y}Co_yB$ ribbons measured in magnetic field at 1 kOe. (b) Magnetization as a function of magnetic field for $(Nd_{0.8}Ce_{0.2})_2Fe_{14-y}Co_yB$ melt spun ribbons measured at 300 K. (c) Magnetization as a function of magnetic field of $(Nd_{0.5}Ce_{0.5})_2Fe_{14-y}Co_yB$ melt spun ribbons measured at 300 K. (d) Intrinsic coercivity, Hci, maximum energy product, (BH)max, and remanence magnetization Br as functions of temperature for melt spun ribbons of both $(Nd_{0.8}Ce_{0.2})_2Fe_{14}Co_2B$ (open symbols),and $(Nd_{0.5}Ce_{0.5})_2Fe_{13}CoB$ (solid symbols).

magnetic field demonstrates that T_C increases nearly linearly with the Co substitution (Fig. 4a and inset). For example, two Co atoms per formula unit substituted for Fe increase T_C by ~150 K to 695 K. The low temperature anomaly at T~310 K disappears for y ≥ 1 (Fig. 4a). We believe that the disappearance of the low temperature anomaly in Co-containing alloys is due to suppression of phase separation, which was observed in Co-free $(Nd_{2-x}Ce_x)_2Fe_{14}B$ with 0.20 ≤ x ≤ 0.30 [20]. The magnetization measured as a function of magnetic field at 300 K shows that the Co addition not only increases T_C, but it also helps to make a nearly perfect square-shaped demagnetization curve that ultimately enhances the other magnetic properties such as (BH)max, and it is the best for y = 2 (Fig. 4b). Theoretical calculations have shown that the Co atoms preferentially substitute for Fe in the Fe (4c) position in the $Ce_2Fe_{14}B$ alloy [23]. The deterioration of the magnetic properties with more than two Co atoms per formula unit in $(Nd_{0.8}Ce_{0.2})_2Fe_{14-y}Co_yB$ may be due to the additional Co atoms occupying other Fe sites as suggested by Mössbauer, neutron, and NMR [24–27] studies of $Nd_2Fe_{14-x}Co_xB$. The anisotropy field, saturation moment, and remanent magnetization are relatively constant with the substitution of Co for Fe in $(Nd_{0.8}Ce_{0.2})_2Fe_{14-y}Co_yB$ for y up to 2.5.

We have observed that Hci decreases while (BH)max remains practically unchanged for $(Nd_{0.8}Ce_{0.2})_2Fe_{14-y}Co_yB$ with Co concentration 0 ≤ y ≤ 1.5. For 1.5 < y ≤ 2, both Hci and (BH)max increase, and the maximum values are 7.8 kOe and 16 MGOe, respectively, for Hci and (BH)max at y = 2. Both begin to decrease when Co concentration increases beyond 2 (not shown in Fig. 4). Interestingly, the addition of 2.5 wt.% ZrC to the $(Nd_{0.8}Ce_{0.2})_2Fe_{12}Co_2B$ further increases the Hci by 15% (9 kOe) and (BH)max by 6% (17 MGOe) (not shown in Fig. 4), which are higher than the 20% Dy substitution (5.2 wt.%) $(Nd_{0.8}Dy_{0.2})_{10}Fe_{84}B_6$ melt spun ribbons (Hci = 8.8 kOe, (BH)max = 15.8 MGOe at 300 K (no high temperature data were available) [28]. The enhanced magnetic properties with the addition of ZrC are due to the microstructure modification by enhancing the quenchability and significantly refining the grain size [5].

We have also studied the effect of Co substitution for the higher Ce concentration alloy: $(Nd_{0.5}Ce_{0.5})_2Fe_{14-y}Co_yB$. The magnetization as a function of magnetic field is shown in Fig. 4c. One Co atom per formula unit substituted for Fe significantly increases Hci and (BH)max, and the B vs H loop is nearly square shaped compared to the cobalt-free sample. A further increase of Co concentration decreases Hci. The room temperature Hci, (BH)max, Br, and T_C for $(Nd_{0.5}Ce_{0.5})_2Fe_{14}B$ were found to be 4.9 kOe, 9.5 MGOe, 8.2 kG, and 520 K, respectively, which are lower than those of $Nd_2Fe_{14}B$ alloy. The values of Hci, (BH)max, Br, and T_C increase to 8 kOe, 14.6 MGOe, 8.2 kG, 590 kOe for 1 Co atom per formula unit substituted for Fe in $(Nd_{0.5}Ce_{0.5})_2Fe_{13}Co_1B$. These values are close to those of Dy-free $Nd_2Fe_{14}B$. Most importantly, the amount of Nd, one of the critical elements, is reduced by ~50 wt.%, making the alloy less costly than the parent compound. Further, considering current metal prices, the cost of components in the Ce, Co co-doped alloys varies between ~$15 and ~$27/kg depending on composition, while the same for $Nd_2Fe_{14}B$ + 2% Dy alloy is ~$33/kg. Our studies of Co substitution in $(Nd_{1-x}Ce_x)_2Fe_{14-y}Co_yB$ show that the critical concentration of Co that provides the best magnetic properties depends on the amount of Ce present in the sample.

Comparing the high temperature properties of both $(Nd_{0.8}Ce_{0.2})_2Fe_{12}Co_2B$ and $(Nd_{0.5}Ce_{0.5})_2Fe_{13}CoB$, Hci of both alloys are close to each other, and they vary from ~8 kOe at 300 K to ~3 kOe at 500 K with the temperature coefficient β of –0.32% K^{-1} (Fig. 4d). However, (BH)max of the former alloy (20% Ce, 2 Co atoms per formula unit) is higher by 11%, and 44% at 300 K, and 500 K, respectively, compared to that of the latter alloy (50% Ce, 1 Co atom per formula unit). Br of $(Nd_{0.8}Ce_{0.2})_2Fe_{12}Co_2B$ is almost identical to that of $(Nd_{0.5}Ce_{0.5})_2Fe_{13}CoB$ at 300 K, but the latter is lower by 25% at 500 K. The enhanced (BH)max is likely due to a synergistic effect between the mixed valence Ce and adjacent Co atoms [23,29], which results in a nearly square hysteresis loop. The obtained values of (BH)max in the Ce, Co co-doped samples are significantly higher compared to the Dy containing $[(Nd_{0.5}Y_{0.25}Dy_{0.25})_{2.2}Fe_{14}B]_{(100-2x)/17.2} + Ti_xC_x$ ((BH)max = ~9 MGOe at 300 K and ~1 MGOe at 548 K, for x = 2) ribbons [5].

4. Conclusions

In summary, we have investigated the permanent magnetic properties of both bulk polycrystalline drop cast alloys, and nanocrystalline melt-spun ribbons of Ce and Co co-doped Nd–Fe–B based alloys, which are comparable to many of the Dy doped $Nd_2Fe_{14}B$-based grades of permanent magnets. The substitution of Ce for Nd drops the Curie temperature T_C by 19% from 580 K ($Nd_2Fe_{14}B$) to 472 K ($Ce_2Fe_{14}B$). But cobalt substituting for optimally doped with Ce in $(Nd_{1-x}Ce_x)_2Fe_{14}B$ alloy increases T_C. The room temperature values of Hci, (BH)max, and T_C for $(Nd_{0.8}Ce_{0.2})_2Fe_{12}Co_2B$ and $(Nd_{0.5}Ce_{0.5})_2Fe_{13}CoB$ alloys are 7.7 kOe, 16 MGOe, 695 K, and 8 kOe, 14.6 MGOe, 590 K, respectively. The cost of Ce, Co co-doped materials is significantly lower compared to the $Nd_2Fe_{14}B$ + 2%Dy, and $Nd_2Fe_{14}B$ + 4% Dy permanent magnets. Furthermore, the replacement of the Nd (also an energy critical element) by Ce (an inexpensive, abundant, non-critical metal) also helps alleviate the Nd shortage.

Acknowledgments

This work was supported by the U.S. Department of Energy (DOE), Advanced Research Projects Agency-Energy (ARPA-E), Rare Earth Alternatives in Critical Technologies for Energy (REACT). The research was performed at the Ames Laboratory which is operated for the U.S. DOE by Iowa State University under contract #DE-AC02-07CH11358. The authors would like to acknowledge Wareen Straszheim for taking microprobe WDS data.

References

[1] J.F. Herbst, J.J. Croat, F.E. Pinkerton, W.B. Yelon, Phys. Rev. B 29 (1984) 4176.
[2] W.C. Chang, S.H. Wu, B.M. Ma, C.O. Bounds, J. Magn. Magn. Mater. 167 (1997) 65.
[3] K. Hirota, H. Nakamura, T. Minowa, M. Honshima, IEEE Trans. Magn. 42 (2006) 2909.
[4] D.J. Branagan, R.W. McCallum, J. Magn. Magn. Mater. 146 (1995) 89.
[5] W. Tang, Y.Q. Wu, K.W. Dennis, M.J. Kramer, I.E. Anderson, R.W. McCallum, J. Appl. Phys. 99 (2006) 08B510.
[6] Zhongmin Chen, Y.Q. Wu, M.J. Kramer, B.R. Smith, B. Ma, M. Huang, J. Magn. Magn. Mater. 268 (2004) 105.
[7] X.B. Liu, Z. Altounian, M. Huang, Q. Zhang, J.P. Liu, J. Alloys. Comp. 549 (2013) 366.
[8] J. Chaboy, N. Plugaru, J. Bartolome, G. Subas, Phys. Rev. B 67 (2003) 014415.
[9] W. Gong, Q. Li, L. Yin, J. Appl. Phys. 69 (1991) 5512.
[10] M. Zhu, W. Li, J. Wang, L. Zheng, Y. Li, K. Zhang, H. Feng, T. Liu, IEEE Trans. Magn. 58 (2014) 1000104.
[11] Z.B. Li, B.G. Shen, M. Zhang, F.X. Hu, J.R. Sun, J. Alloys Comps 628 (2015) 325.
[12] C. Yan, S. Guo, R. Chen, D. Lee, A. Yan, IEEE Trans. Magn. 50 (2014) 2104604.
[13] M.Y. Xing, J.Z. Han, Z. Lin, F.M. Wan, C. Li, S.Q. Liu, C.S. Wang, J.B. Yang, Y.C. Yang, J. Magn. Magn. Mater. 331 (2013) 140.
[14] E.J. Skoug, M.S. Meyer, F.E. Pinkerton, M.M. Tessema, D. Haddad, J.F. Herbst, J. Alloys Comps 574 (2013) 552.
[15] E. Niu, Z.A. Chen, G.A. Chen, Y.G. Zhao, J. Zhang, X.L. Rao, B.P. Hu, Z.X. Wang, J. Appl. Phys. 115 (2014) 113912.
[16] Z.B. Li, B.G. Shen, M. Zhang, F.X. Hu, J.R. Sun, J. Alloys Comps 618 (2015) 325.
[17] C. Yan, S. Guo, R. Chen, D. Lee, A. Yan, IEEE Trans. Magn. 50 (2014) 2102605.
[18] C.D. Fuerst, J.F. Herbst, E.A. Alson, J. Magn. Magn. Mat. 567 (1986) 54.
[19] A.K. Pathak, M. Khan, K.A. Gschneidner Jr., R.W. McCallum, L. Zhou, K. Sun, K.W. Dennis, C. Zhou, F.E. Pinkerton, M.J. Kramer, V.K. Pecharsky, Adv. Mater 27 (2015) 2663.
[20] K.A. Gschneidner Jr., R.W. Mccallum, M. Khan, A.K. Pathak, V.K. Pecharsky, L. Zhou, K. Sun, K.W. Dennis, M.J. Kramer, D. Brown, C. Zhou, G.C. Hadjipanayis, C.H. Chen, J.P. Liu (Eds), Proceedings 23rd International Workshop on Rare Earth

and Future Permanent Magnets and Their Applications (REPM 2014), August 17-21, 2014, pp. 403–406, Annapolis, Maryland, USA.
[21] Z.B. Li, M. Zhang, B.G. Shen, J.R. Sun, Appl. Phys. Lett. 102 (2013) 102405.
[22] C.B. Rong, D. Wang, V.V. Nguyen, M. Daniil, M.A. Willard, Y. Zhang, M.J. Kramer, P. Liu, J. Phys. D. Appl. Phys. 46 (2013) 045001.
[23] A. Alam, D.D. Johnson, Phys. Rev. B 89 (2014) 235126.
[24] D.H. Ryan, Z. Altounian, J.O. Strom-Olsen, W.B. Muir, Phys. Rev. B 39 (1989) 4730.
[25] P. Deppe, M. Rosenberg, S. Hirosawa, M. Sagawa, J. Appl. Phys. 61 (1987) 4337.
[26] J.F. Herbst, W.B. Yelon, J. Appl. Phys. 60 (1986) 4224.
[27] L.X. Liao, Z. Altounian, D.H. Ryan, Phys. Rev. B 47 (1993) 11230.
[28] Z. Liu, D. Qian, D. Zeng, IEEE Trans. Magn. 48 (2012) 2797.
[29] A. Alam, M. Khan, R.W. McCallum, D.D. Johnson, Appl. Phys. Lett. 102 (2013) 042402.